Detection and 3D localization of ultralight aircrafts and drones with a WiFi-based Passive Radar

T. Martelli, F. Murgia, F. Colone, C. Bongioanni, P. Lombardo

DIET Dept., Sapienza University of Rome
Via Eudossiana, 18 – 00184 Rome, Italy
{tatiana.martelli, fabiola.colone, carlo.bongioanni, pierfrancesco.lombardo}@uniroma1.it

Keywords: Passive Radar, WiFi signals, aircraft detection, drones detection, 3D localization.

Abstract

This paper investigates the possibility to localize small aircrafts and drones in three-dimensions by exploiting a passive radar based on WiFi transmissions. Specifically, following the latest results of the authors, where the effectiveness of the WiFi-based passive radar has been demonstrated for the detection and 2D localization of small aircrafts, the advanced capability to estimate their height is demonstrated in this paper. In addition, the new capability is explored to detect and localize small commercial drones and UAVs in 3D. The experimental results achieved by means of a demonstrator developed at Sapienza University of Rome support the practical applicability of WiFi-based passive radar for improving security of small airfields and outdoor areas.

1 Introduction

In the recent years, there was a growing use of drones and Unmanned Aerial Vehicles (UAV) due to their low cost, increased utility and ease of handling. Their widespread availability for a wide variety of applications has redefined the security risks of critical infrastructures, national borders and military bases. Consequently, detection, tracking and classification of these very small and low flying objects have become key requirements. To this purpose, many active radars operating at X and Ku bands have been specifically designed as anti-drone and/or anti-UAV surveillance systems. These systems may be used in urban and remote areas and are able to detect the considered targets in all weather conditions, [1]-[2].

A compelling alternative to the use of active radar is represented by passive radar (PR) systems. PR exploits existing transmitters as illuminators of opportunity to perform target detection and localization. Since they do not require a dedicated transmitter, these sensors offer a number of interesting advantages such as low cost, reduced energy consumption and covert operation, especially useful for anti-terrorism or military applications. Moreover, due to fact that they do not generate additional electromagnetic radiations, they are usually referred to as green systems and are especially interesting for urban area monitoring, [3]. As an example, the feasibility of the PR sensor for detection of drones and small UAVs has been investigated in [4]-[6] using GSM, communication signals and digital television signals as illuminators of opportunity.

Aiming at short range surveillance applications, the opportunistic exploitations of transmissions for networking (WiFi, WiMAX, LTE) is especially attractive since they have been proliferating at a rapid rate for both commercial and private use. Among them, the WiFi transmissions represent an attractive solution. Indeed these are widely accessible sources of opportunity, able to provide wide bandwidth (and therefore range resolution) and well-controlled signals. Recently, such sources have been considered in PR systems for small airport surveillance, [7]. In particular, the experimental tests performed in a small private airfield for light/ultralight airplanes have shown that the WiFi-based PR is able to correctly detect and accurately localize (on the 2D plane) small and ultralight aircrafts moving on the runway and in the surrounding areas. Moreover, the possibility to jointly exploit the WiFi-based PR developed by Sapienza University of Rome and a Ku-band FMCW developed by MetaSensing for the enhancement of the security level in small airports has been considered in [8].

This paper aims at extending the results shown in [7]-[8]. First, the possibility to retrieve the height of the detected aircrafts by exploiting multiple receiving antennas is investigated. In particular, by employing a set of three antennas that have both horizontal and vertical displacement, an interferometric approach can be exploited to estimate both the azimuth and the elevation angles of the target echoes. This allows a full localization in three-dimensions. In addition, aiming at extending the range of possible applications of the WiFi-based PR, the detection of drones has been explored. To this purpose, a dedicated acquisition campaign has been performed in a small external area of the Sapienza University sport facility using a very low RCS drone as a cooperative target. The obtained results show that the passive sensor is able to detect drones along their trajectory. Moreover, its azimuth and elevation angles have been estimated allowing to localize them in three-dimensions.

The paper is organized as follows. The employed receiver set-up together with the main processing steps for target detection and 3D localization are reported in Section 2. The obtained results against ultralight aircrafts are illustrated in Section 3, while the performed test campaign and its results for drone targets are shown in Section 4. Finally, our conclusions are drawn in Section 5.

2 WiFi-based passive radar system

In [7]-[8] we have shown that by exploiting the range and azimuth measurements provided by the two horizontally displaced surveillance antennas, it is possible to localize the target on the 2D Cartesian plane. In principle, by exploiting an additional surveillance antenna displaced in the vertical direction, even the elevation angle of the target can be estimated, which allows us to measure its height from ground. This is illustrated in the following. In particular, the used WiFi-based PR experimental set-up, together with the processing scheme for target detection and 3D location, are reported in Figure 1 and briefly described below.

A commercial WiFi access point (AP) was used as transmitter of opportunity, set up to emit a beacon signal exploiting a DSSS modulation with a 3 ms repetition interval. Its output is connected to the transmitting antenna (TX) through a directional coupler, which spills a fraction of the signal that is digitized by the first receiving channel of the PR receiver, to be used as the reference signal for the subsequent processing. In particular, the experimental WiFi-based, quad-channel PR receiver developed at Sapienza University of Rome and reported in [9] has been employed. Three commercial WiFi panel antennas have been used to collect the surveillance signals as reported in Figure 1(a). Specifically, the first surveillance antenna (RX1) was mounted above the second and third ones (RX2 and RX3) in a quasi-monostatic configuration with respect the TX. The horizontal displacement between RX2 and RX3 was set to d_{23}=12 cm while the vertical displacement between RX1 and RX2/RX3 was equal to d_{12}=d_{13}=40 cm. Depending on the considered test campaign, the TX was mounted either just above or on the right of the surveillance antennas as illustrated in Figure 1(a). All the employed antennas are characterized by a gain of 12 dBi, a front-to-back ratio of 15 dB and beam widths equal to about 80° and 23° on the horizontal and the vertical plane, respectively.

After a fully coherent base-band down-conversion stage, all the signals are sampled at 22 MHz and stored for off-line processing. Successively, they are processed by the WiFi-based PR processing scheme illustrated in Figure 1(b). First, sidelobes control techniques are applied on the reference signal to mitigate the high structures appearing in the Ambiguity Function (AF) in the range dimension due to the adopted modulation scheme. Then, a disturbance cancellation stage is performed to remove the undesired contributions (above all the direct signal breakthrough and multipath or clutter echoes) received together with the moving target echo on the surveillance channels. To this purpose, the sliding version of the Extensive Cancellation Algorithm (ECA-S) is considered, [10]. With respect to the standard ECA, it was shown in [10] that its sliding version makes the WiFi-based PR more robust to the slowly varying characteristics of the environment and, at the same time, it preserves the low-Doppler moving target thus improving the detection performance of the resulting system. After the above stages, target detection is sought by evaluating the bistatic range-velocity map over the desired coherent

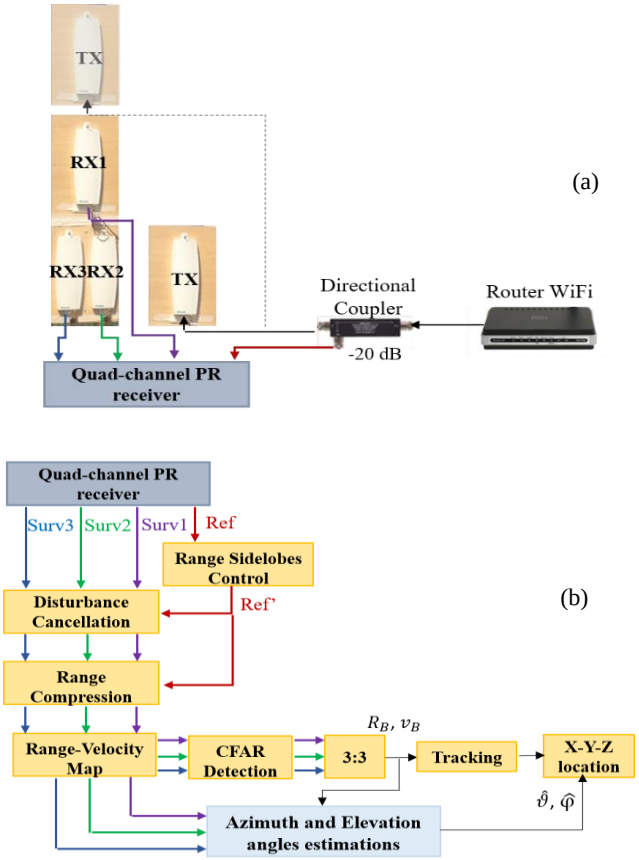

Figure 1. WiFi-based PR: (a) receiver setting and (b) processing scheme for target detection and 3D localization.

processing interval (CPI). A Cell-Average Constant False Alarm Rate (CA-CFAR) threshold is applied to the obtained map to automatically detect targets over the bistatic range/velocity plane with a nominal probability of false alarm P_{fa}, [11]. In this case, a three-out-of- three detection criterion has been adopted. A conventional Kalman tracking algorithm could also be applied after this stage to reduce the false alarms while yielding more accurate range/velocity measurements.

Possible limitations to the WiFi-based PR operation at these stages might be due to interference from other APs used in the same area. However, if the interfering source operates on adjacent or overlapped frequency channels, its transmission is expected to yield just a limited increase in the system noise floor. This can be explained by observing that (i) the received interfering signal does not correlate with the reference signal adopted for matched filtering, and (ii) the probability of collision between the same pair of APs is usually low. Differently, when the interfering sources operate in the same WiFi channel used by the AP of opportunity, the occurrences of collisions are substantially avoided thanks to the implementation of carrier sense multiple access (CSMA) protocols. Therefore, the effect of an interfering AP would be to inhibit a high rate transmission of pulses by the AP of opportunity. This can yield a highly variable temporal separation among consecutive pulses, which in turn can be responsible for high sidelobes along the Doppler dimension of

the ambiguity function. To compensate this behaviour, effective adaptive tapering functions have been designed to automatically control the undesired Doppler sidelobes [12]. Therefore, until the traffic load of the channel is not very high, the system performs nicely, whereas the performance is expected to degrade under high traffic load conditions where the rate of beacon transmission becomes very low.

Once a target has been detected, the phase difference among the surveillance antennas can be evaluated, as a basis to estimate the azimuth (φ) and elevation (θ) angles of the target echo. In particular, a Cartesian coordinate system has been adopted assuming that the three surveillance antennas are located at the points of coordinates $\mathbf{\Omega_{RX1}}=(0,0,z_{RX1})=(0,0,d_{12})$, $\mathbf{\Omega_{RX2}}=(x_{RX2},0,0)=(\frac{d_{23}}{2},0,0)$ and $\mathbf{\Omega_{RX3}}=(x_{RX3},0,0)=(-\frac{d_{23}}{2},0,0)$. After few simple steps, we can write the phase difference, $\Delta\Phi_{ij}$, between RX_i and RX_j as:

$$\Delta\Phi_{23}=\frac{2\pi}{\lambda}(x_{RX2}-x_{RX3})\cos\theta\sin\varphi \quad (1)$$

$$\Delta\Phi_{12}=-\frac{2\pi}{\lambda}(z_{RX1}\cdot\sin\theta+x_{RX2}\cdot\cos\theta\sin\varphi) \quad (2)$$

$$\Delta\Phi_{13}=-\frac{2\pi}{\lambda}(z_{RX1}\cdot\sin\theta+x_{RX3}\cdot\cos\theta\sin\varphi) \quad (3)$$

By solving the above system, we obtain:

$$\theta=\sin^{-1}\left\{-\frac{\lambda}{2\pi\cdot z_{RX1}}\left[\Delta\Phi_{12}+\frac{x_{RX2}\cdot\Delta\Phi_{23}}{(x_{RX2}-x_{RX3})}\right]\right\} \quad (4)$$

$$\varphi=\sin^{-1}\left\{\frac{\lambda}{2\pi\cdot\cos\theta}\cdot\frac{\Delta\Phi_{23}}{(x_{RX2}-x_{RX3})}\right\} \quad (5)$$

Denoting with R_B the bistatic range of the detected target, the target coordinates (x_T,y_T,z_T) can be estimated as follow:

$$\begin{cases}x_T=\frac{R_B}{2}\cdot\cos\theta\sin\varphi\\ y_T=\frac{R_B}{2}\cdot\cos\theta\cos\varphi\\ z_T=\frac{R_B}{2}\cdot\sin\theta\end{cases} \quad (6)$$

From the retrieved z_T coordinate, taking also into account the height of the surveillance antennas from the ground, the height from ground of the detected target can be easily obtained.

3 Aircrafts 3D localization: Experimental results

In this section, experimental results are shown against ultra-light aircrafts. To demonstrate the effectiveness of the 3D localization, a test campaign has been performed in a small airfield named "Aviosuperficie Monti della Tolfa" located in Santa Severa (about 60 km North of Rome). It is composed by a single runway, 520 meters long and 20 meters wide, with a grass surface (see Figure 2). More details on the airfield are reported in [7]-[8]. In the considered experiment, the TX antenna was mounted at a height of about 2.20 meters from ground, about 38 cm above the RX1 antenna. Aiming at detecting the small aircrafts during their taking-off/landing operations, all the surveillance antennas were pointed at 345° w.r.t. North.

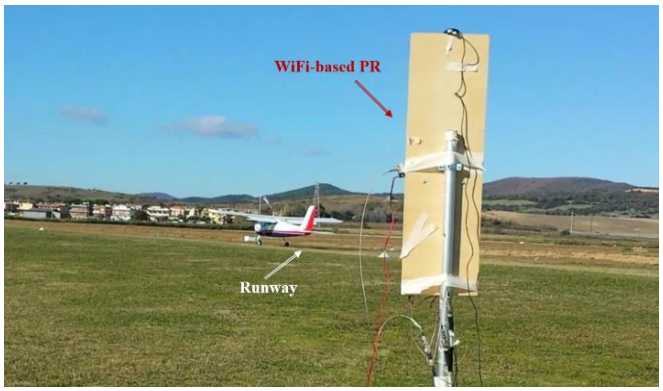

(a)

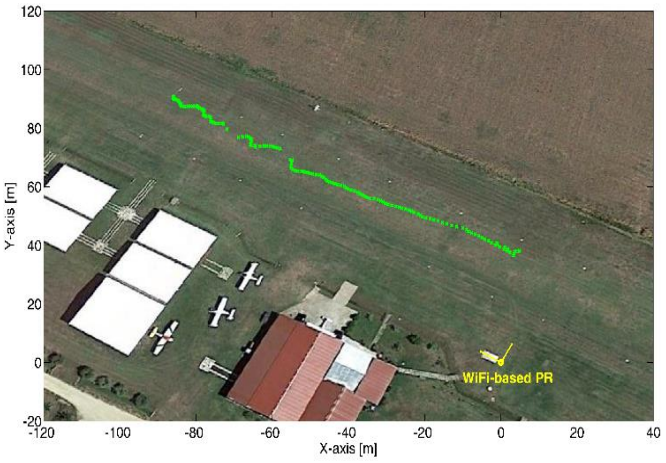

(b)

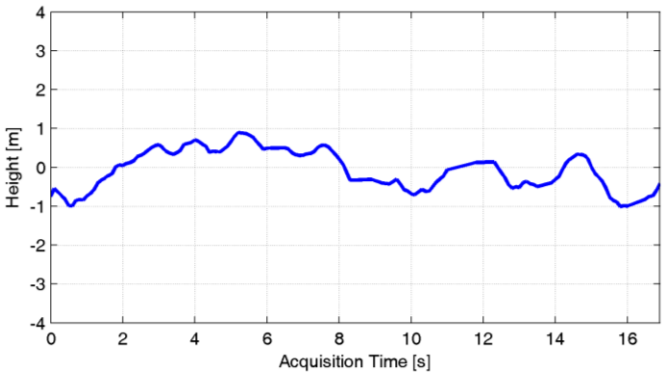

(c)

Figure 2. Test against an aircraft moving on the runway: (a) picture of the performed test; (b) localization results on the XY plane; (c) target height estimation versus acquisition time.

The signal processing stages illustrated in Figure 1(b) have been applied to the collected surveillance signals. The ECA-S algorithm is applied over a range of 600 m with a batch duration equal to 100 ms, whereas the filter update rate is set to be equal to the AP beacon emission rate. Thereafter, the bistatic range-velocity map is evaluated using a CPI=0.3 s over consecutive portions of the acquired signal with a fixed displacement of 0.1 s. A CFAR threshold is applied to the individual range-velocity map set to provide $P_{fa}=10^{-2}$, which allows a nominal $P_{fa}=10^{-6}$ for the final range-velocity plane, since a three out of three criterion is adopted to integrate the detection results obtained at the three surveillance channels. Then, once a target has been detected, its azimuth and elevation angles are measured.

Unfortunately, for the considered tests, the targets were not equipped with a GPS receiver. Therefore, to illustrate preliminarily the capability to measure the target height above ground, we first report the results of a test performed against a ultralight aircraft moving on the runway during the receiver registration of 17 s (see Figure 2(a)). In detail, it was a two-seat airplane with length of about 7 meters, height of 2 meters and wingspan of 10 meters. The obtained localization results in the XY plane are shown in Figure 2(b). We observe that the small aircraft is detected continuously along its trajectory up to a distance of about 100 meters. Obviously, the target localization accuracy degrades as the aircraft gets far away from the PR receiver. Figure 2(c) shows the estimated target height above ground as a function of the acquisition time. We observe that the obtained measurements are well in line with the test geometry; in fact, they are approximately equal to zero meters, the actual fluctuating values giving a direct idea of the achievable height estimation error.

(a)

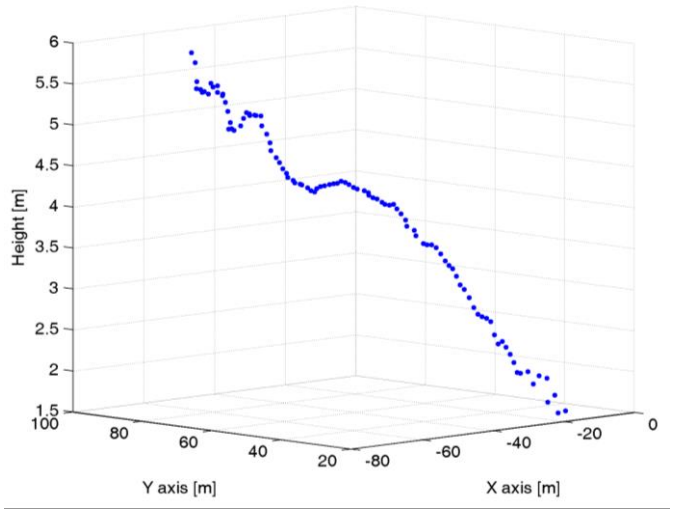

(b)

Figure 3. Test against a taking off aircraft: (a) picture of the performed test; (b) 3D localization results.

As a second test, we report the results of the same aircraft during its phase of take-off (see Figure 3(a)). The 3D localization result is shown in Figure 3(b). As is apparent, the small aircraft is correctly detected while flying over the runway up to a distance of about 90 meters. Moreover, while the aircraft flies away from the PR receiver, the measured height increases up to 6 meters. In fact, given the considered test geometry, we are able to detect aircrafts flying to few meters above ground.

4 Detection and 3D localization against drones: Experimental results

The potentiality of the considered system is here investigated for the detection and localization of drones characterized by very low RCS.

To this purpose, a test campaign has been conducted in the external area of the University sport center named CUS, in Rome. A sketch of the test area together with the WiFi-based PR receiver location is illustrated in Figure 4(a). Specifically, the considered area is constituted mostly of grass surface and it is approximately 40 meters long and 9 meters wide. A very small drone is used as cooperative target (see Figure 4(b)). It is made of carbon fiber and expanded foam and has size 60 cm x 60 cm x 9 cm. A sketch of the geometry for one of the performed test is depicted in Figure 4(c). Notice that, in this case, the TX antenna is mounted on the right of the surveillance antennas at a distance of 48 cm with respect to RX2. Both TX and RX2/RX3 are mounted at a height of about 0.85 meters from ground.

Different tests have been performed and all the acquired data have been processed with the whole processing scheme shown in Figure 1(b). The ECA-S has been applied for a range of 400 m with batch duration set to 500 ms and filter update rate equal to the AP beacon emission rate. A CPI=0.5 s is used to evaluate the range-velocity map on each surveillance channel over consecutive portions of the acquired signals with a fixed displacement of 0.1 s. Then a CA-CFAR with $P_{fa}=10^{-1.3}$ is adopted on the single channel and a three out three detection criterion across the three surveillance antennas is used allowing a $P_{fa}=10^{-4.}$ The results of two different acquisitions are reported below, where the drone is remotely piloted to fly specified test

trajectories that are intended to emulate typical drone usage profiles.

In the first one, the drone soars from point A (see Figure 4(a)), at a distance of about 20 meters from the PR sensor. The raw detection results over the range-velocity plane collected during the whole acquisition time (about 10 sec) are reported with 'x' markers in Figure 5(a). As it is apparent, a cloud is visible at a bistatic range of about 40 meters. These detections correspond to the target returns since they are clearly compliant with the test geometry. Instead, the isolated markers are false alarms due to thermal noise and disturbance residuals that can be discarded easily by a tracking algorithm as illustrated in the following. In the second test, the drone moves from point B (Figure 4(a)), at about 30 m from the PR sensor, toward the receiver location going up and down. The corresponding detection results are reported in Figure 5(b). It is evident that also in this case the drone has been successively detected along its trajectory despite its small dimensions. In both Figure 5(a) and Figure 5(b), the output of a Kalman tracking filter operating in the range-velocity plane is also reported. Specifically, the sequence of red plots represents the range-velocity estimations associated to the considered target. Then, the phase difference among the surveillance antennas at the target detection point is exploited to evaluate the azimuth and elevation angles.

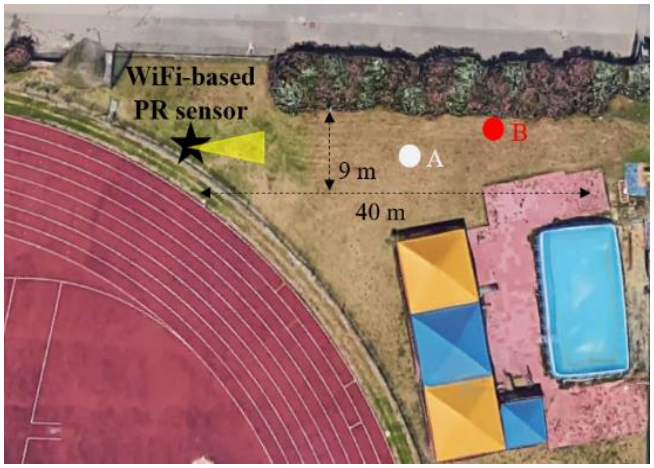

(a)

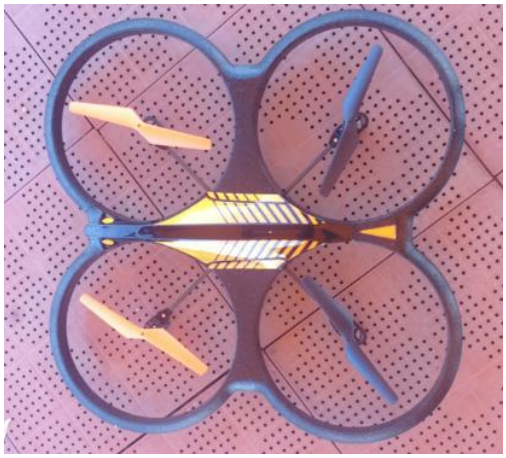

(b)

(c)

Figure 4. Scenario of the test campaign against drones: (a) sketch of the test area; (b) picture of the used drone; (c) sketch of a performed test.

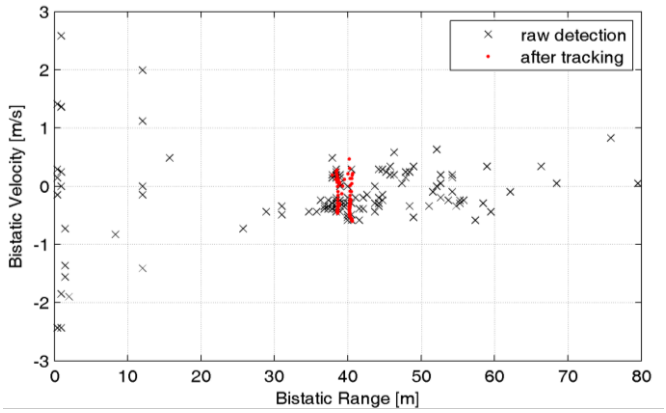

(a)

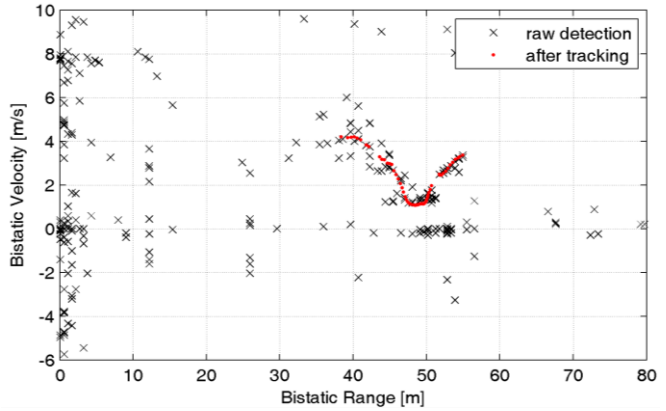

(b)

Figure 5. Detection results over the Range-Velocity plane for two different tests against drones.

The corresponding 3D localization results are shown in Figure 6. As it is evident, the accuracy of the sensor is lower when operating against drone targets than it was against the small aircrafts. However, although the ground truth is not available, in both tests we observe that the results are in line with the previously described drone maneuvers and appear very well

consistent. Even more continuous tracks could be obtained by applying an additional tracking stage in the Cartesian plane to follow the evolution of the x,y,z coordinates.

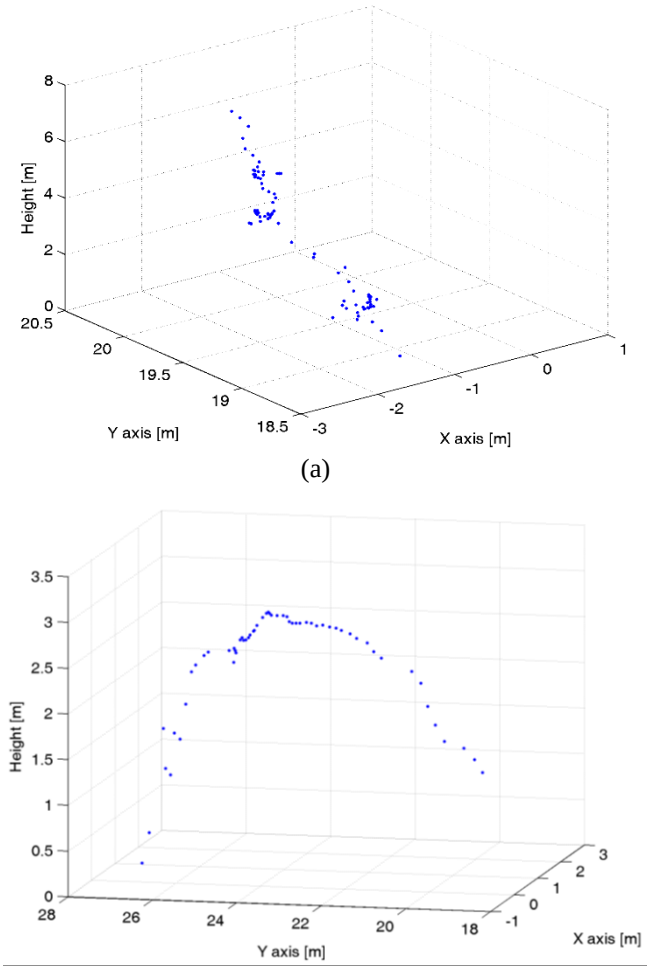

(a)

(b)

Figure 6. 3D localization results for the tests in Figure 5(a)-(b), respectively.

5 Conclusions

In this paper, the advanced capability has been investigated of localizing in three dimensions ultra-light aircrafts and drones by means of a short-range PR based on the WiFi router emissions. First, following the latest results shown in [7]-[8], where the effectiveness of the considered sensor was demonstrated for the detection and 2D localization of small aircrafts, a demonstration is given of the capability to estimate their height from the ground by exploiting multiple surveillance antennas. Thereafter, the WiFi-PR capability to detect and localize drones within short ranges has been investigated. To this purpose, a dedicated acquisition campaign has been performed using a very low RCS drone as cooperative target that is piloted to fly desired trajectories. The obtained results show that the passive sensor is able to correctly detect and localize in 3D the small flying object along its trajectory. The reported experimental results support the practical applicability of the WiFi-based PR concept for such advanced security applications as a viable alternative to active sensors at least in the short range. Further investigations and possibly the joint exploitation of different types of signal sources can be useful to extend the range of the surveillance capability.

References

[1] http://www.advancedradartechnologies.com/products-services/art-drone-sentinel.

[2] www.kelvinhughes.com/security/uav-drone-detection.

[3] P. Howland, Special Issue on Passive Radar Systems – *IEEE Proceedings on Radar, Sonar and Navigation*, vol. 152, no. 3, pp. 105-106, 3 June 2005.

[4] B. Knoedler, R. Zemmari, W. Koch, “On the detection of small UAV using a GSM passive coherent location system”, *2016 17th International Radar Symposium (IRS)*, Krakow, 2016, pp. 1-4.

[5] X. Yang, K. Huo, W. Jiang, J. Zhao, Z. Qiu, “A passive radar system for detecting UAV based on the OFDM communication signal”, *2016 Progress in Electromagnetic Research Symposium (PIERS)*, Shanghai, 2016, pp. 2757-2762.

[6] Y. Liu, X. Wan, H. Tang, J. Yi, Y. Cheng and X. Zhang, "Digital television based passive bistatic radar system for drone detection," *2017 IEEE Radar Conference (RadarConf)*, Seattle, WA, USA, 2017, pp. 1493-1497.

[7] F. Colone, T. Martelli, C. Bongioanni, D. Pastina and P. Lombardo, "WiFi-based PCL for monitoring private airfields," in *IEEE Aerospace and Electronic Systems Magazine*, vol. 32, no. 2, pp. 22-29, February 2017.

[8] T. Martelli, C. Bongioanni, F. Colone, P. Lombardo, L. Testa and A. Meta, "Security enhancement in small private airports through active and passive radar sensors," *2016 17th International Radar Symposium (IRS)*, Krakow, 2016, pp. 1-5.

[9] A. Macera, C. Bongioanni, F. Colone, and P. Lombardo, "Receiver architecture for multi-standard based Passive Bistatic Radar," *2013 IEEE Radar Conference (RadarCon13)*, Ottawa, ON, 2013, pp. 1-5.

[10] F. Colone, C. Palmarini, T. Martelli, E. Tilli, "Sliding extensive cancellation algorithm for disturbance removal in passive radar," in *IEEE Transactions on Aerospace and Electronic Systems*, vol. 52, no. 3, pp. 1309-1326, June 2016.

[11] F. Colone, P. Falcone, C. Bongioanni, and P. Lombardo, "WiFi-Based Passive Bistatic Radar: Data Processing Schemes and Experimental Results," *in IEEE Transactions on Aerospace and Electronic Systems*, vol. 48, no. 2, pp. 1061-1079, APRIL 2012.

[12] P. Falcone, F. Colone, P. Lombardo, “Doppler Frequency Sidelobes Level Control for WiFi-Based Passive Bistatic Radar”, IEEE Radar Conference 2011, 23-27 May, 2011, Kansas City, Missouri (USA), pp. 435-440.